Ultrasonics Sonochemistry 21 (2014) 2037–2043

Contents lists available at ScienceDirect

Ultrasonics Sonochemistry

journal homepage: www.elsevier.com/locate/ultson

Acoustic power dependences of sonoluminescence and bubble dynamics

Hyang-Bok Lee, Pak-Kon Choi *

Department of Physics, Meiji University, 1-1-1 Higashimita, Tama-ku, Kawasaki 214-8571, Japan

ARTICLE INFO

Article history:
Received 10 December 2013
Received in revised form 10 February 2014
Accepted 11 February 2014
Available online 20 February 2014

Keywords:
Sonoluminescence
Sonochemiluminescence
Bubble streamer
Bubble cluster
High-speed photography
Acoustic emission

ABSTRACT

The decreasing effect of sonoluminescence (SL) in water at high acoustic powers was investigated in relation to bubble dynamics and acoustic emission spectra. The intensity of SL was measured in the power range of 1–18 W at 83.8 kHz for open-end (free liquid surface and film-covered surface) and fixed-end boundaries of sound fields. The power dependence of the SL intensity showed a maximum and then decrease to zero for all the boundaries. Similar results were obtained for sonochemiluminescence in luminol solution. The power dependence of the SL intensity was strongly correlated with the bubble dynamics captured by high-speed photography at 64 k fps. In the low-power range where the SL intensity increases, bubble streamers were observed and the population of streaming bubbles increased with the power. At powers after SL maximum occurred, bubble clusters came into existence. Upon complete SL reduction, only bubble clusters were observed. The subharmonic in the acoustic emission spectra increased markedly in the region where bubble clusters were observed. Nonspherical oscillations of clustering bubbles may make a major contribution to the subharmonic.

1. Introduction

Sonoluminescence (SL) is light emission from a liquid medium exposed to intense ultrasound. A large number of bubbles generated in the liquid undergo repeated expansion and contraction. This produces high-temperature and high-pressure conditions inside the bubbles at bubble collapse, resulting in the emission of acoustic waves and light, and in the decomposition of water molecules into hydroxyl (OH) radicals. In a luminol aqueous solution, luminol reacts with OH radicals at bubble interfaces, emitting bluish light known as sonochemiluminescence (SCL). The SL or SCL intensity depends on experimental parameters such as acoustic power and frequency and on experimental conditions such as the type of acoustic field, the content of dissolved gas, and the solution temperature [1–5].

We focus here on the acoustic-power dependences of SL and SCL intensity, which are important for the basic understanding of cavitation phenomena and also for designing systems for sonochemical applications. The production of OH radicals has been shown to exhibit nonlinear power dependence [6–10]. Henglein and Gutierrez [8] demonstrated that the yield of iodine during KI oxidation due to OH radicals showed a maximum when measured as a function of acoustic power. Negishi [11] reported that the SCL intensity suddenly decreased at an acoustic power of 2 W/cm^2 at 470 kHz. Recently, Hatanaka et al. [12] have observed that the SL intensity decreases at high powers at 132 kHz. They attributed this decreasing effect to the occurrence of bubble clusters from their observation of bubble dynamics at 23 kHz by high-speed photography with a speed of 1000 fps. At high acoustic powers, the vibration or the deformation of sample liquid surface is frequently induced by the acoustic radiation force in the case of an open-type sample container in which acoustic waves are directed towards the liquid surface. The surface vibration or deformation may violate the standing-wave fields, causing a decrease in acoustic pressure. This hypothesis was tested by Lindström [7], who investigated the production of hydrogen peroxide under acoustic-field conditions with free-surface and fixed-surface boundaries. The amount of production saturated at high powers for the fixed-surface boundary and decreased at high powers for the free-surface boundary. Tuziuti et al. [13] reported similar behavior for SCL intensity. No decrease in SCL was observed when the surface was covered with a thin layer of Teflon powder.

The acoustic-power dependences of cavitation events need to be clarified in relation to the bubble dynamics under various conditions of acoustic fields. In the present study, we investigated the power dependences of SL and SCL under three types of acoustic boundary condition at 83.8 kHz: a boundary with a free liquid surface (acoustically open end), a boundary with the surface covered with a thin film (acoustically open end), and a boundary with the surface covered with a stainless-steel plate (acoustically fixed end). The bubble dynamics was observed using high-speed

* Corresponding author. Tel.: +81 44 934 7437; fax: +81 44 934 7911.
E-mail address: pkchoi@isc.meiji.ac.jp (P.-K. Choi).

http://dx.doi.org/10.1016/j.ultsonch.2014.02.008
1350-4177/

photography with a speed of 64 k fps. Acoustic emission spectra were also measured at various powers and their relation to bubble dynamics is discussed.

2. Materials and methods

The experimental setup is shown in Fig. 1. Deionized water or 0.56 mM luminol solution, degassed and saturated with argon, was placed in a rectangular quartz glass cell. The inner size of the cell is 65 mm width, 65 mm depth and 90 mm height. The sample volume was 320 mL. A sandwich-type Langevin transducer with a fundamental frequency of 28 kHz was glued by epoxy resin adhesive to the bottom of the cell. Ultrasonic waves were excited at 83.8 kHz, which is one of the harmonics of the fundamental frequency, using a power amplifier (Electronics & Innovation, 1020L) and a matching transformer. The electric output and reflected powers were displayed by the amplifier, and their difference was used as a measure of the power input to the transducer. The range of the input power used was 1–18 W. The transduction efficiency from electric to acoustic power was measured to be about 61% using the calorimetry method. Luminescence images from the ultrasonic cell were captured using a digital camera (Canon, EOS 6D) with an exposure time of 30 s and a sensitivity of ISO 16,000. The SL intensity was obtained by integrating the brightness over each pixel of whole image using Image-J software.

Three types of liquid-surface boundary were investigated in the SL and SCL measurements. A free-surface boundary and thin-film boundary correspond to an acoustically free end. In the case of the free surface, the liquid surface vibrates at high powers owing to the acoustic radiation force. In the case of the thin-film boundary, the liquid surface was covered with a polyethylene terephthalate (PET) film with a thickness of 0.1 mm, which suppresses the liquid-surface vibration. For the third type of the boundary, 94% of liquid surface area ($63 \times 63\ mm^2$) was covered with a stainless-steel (SUS 304) plate with 17 mm thickness. This thickness is equivalent to a quarter wavelength in SUS 304 at 83.8 kHz, ensuring that the boundary is perfectly rigid and is therefore an acoustically fixed end.

Shadowgraph movies of cavitating bubbles were captured using a high-speed video camera (Shimadzu, HPV-2) with a frame speed of 63 k fps. The sample cell used was the same as that in SC and SCL measurements. We used a zoom lens with a maximum magnification factor of 15 and a working distance of 40 mm. The experimental setup was arranged to achieve the parallel back-illumination of bubbles using a metal halide light source (Sumita Optical Glass, LS-M250) by attaching a glass-fiber guide.

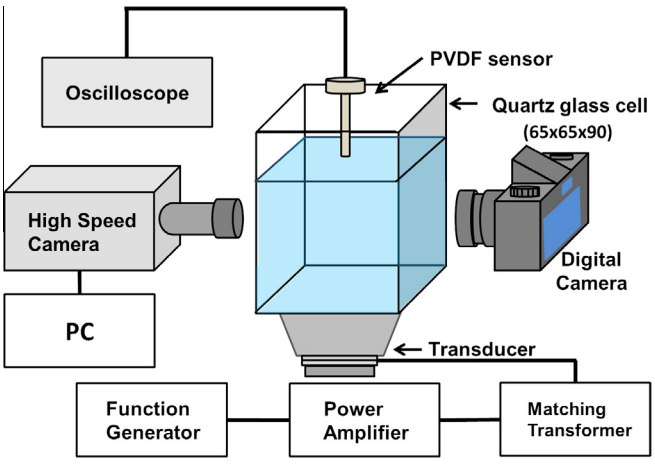

Fig. 1. Experimental setup for measurements of sonoluminescence and high-speed photography. The digital camera is replaced by a glass-fiber light guide when bubble shadowgraphy is carried out.

Acoustic emission signals were detected using a polyvinylidene difluoride (PVDF, 0.1 mm thickness) sensor fabricated in our laboratory. The PVDF film was bonded to the back of a stainless-steel (SUS 304) plate of 5 mm diameter and 0.1 mm thickness. The SUS plate was fixed to a SUS pipe of 5 mm diameter and 100 mm length. The frequency response was flat in the measured frequency range of up to 500 kHz. Measurements were performed by dipping the sensor a few mm into the sample liquid at the center of the cell, while carefully ensuring that no bubbles were trapped on the sensor surface. The detected signals were analyzed using a 4 G Sa/s oscilloscope (Agilent, DSO5052A) incorporating fast Fourier transform (FFT) analysis.

3. Results and discussion

3.1. Power dependences of SL and SCL

Figs. 2 and 3 show captured images of SL and SCL, respectively, for the three types of boundary condition at low, medium, and high powers. For the free surface ((a) in Figs. 2 and 3) and film ((b) in Figs. 2 and 3) boundaries, the spatial distributions of SL and SCL are similar because the liquid surfaces have an acoustically free end. For the SUS-plate boundary ((c) in Figs. 2 and 3), which has an acoustically fixed end, the distribution pattern is different from those for a free end. The images exhibit very complex patterns because of the three-dimensional standing waves in the rectangular container, and the patterns become diffuse at higher powers since bubbles trapped at the antinodes of standing waves move towards the nodes at higher powers. For the film boundary, the SL and SCL intensities were almost quenched at 12 W. Acoustic pressure for the film boundary is possibly larger than that for the free-surface one, because standing-wave fields are disturbed by the deformation of liquid surface and also because a part of the acoustic energy is lost as surface vibration for the free-surface boundary. The surface vibration will be discussed afterward. Measurements of sound fields are needed to make exact comparison of the images for three kinds of boundaries.

The difference between the SL and SCL patterns can be described as follows: the spatial distribution of SCL is wider than that of SL at the same power. SCL is induced by OH radicals that are produced in lower-temperature bubbles, whereas SL is generated from higher-temperature bubbles [14]. This results in a large active-bubble population inducing SCL. The integrated intensity of SL was plotted in Fig. 4 as function of input power for the three types of boundary. For the free-surface boundary, as indicated by solid circles in Fig. 4, the intensity reached a maximum at 9 W and then decreased. The power at which the intensity takes a maximum is abbreviated to "the power of maximum intensity" hereafter. The SL intensity was almost zero at 18 W. For the thin-film boundary, a similar tendency was observed, although the SL reduction occurred at a lower power than for the free-surface boundary. For the SUS plate boundary, the power of maximum intensity and the peak intensity are very sensitive to the position of the SUS plate, i.e., to the degree of interference under the standing-wave condition. We have carefully adjusted the SUS plate position to obtain maximum intensity using a sliding stage. If this adjustment is insufficient, the maximum SL intensity decreases. The power dependence of SL intensity for the SUS plate boundary, however, was essentially the same as those for the free-end boundaries, as indicated in Fig. 4.

The power dependences of SCL intensity are shown in Fig. 5. The intensities exhibited maxima and then decreased to zero, similarly to the SL intensities. This behavior for MBSL was also observed by